Published in final edited form as:

Diabetologia. 2014 June ; 57(6): 1232–1241. doi:10.1007/s00125-014-3212-1.

Muscle-specific activation of Ca^{2+}/calmodulin-dependent protein kinase IV increases whole-body insulin action in mice

Hui-Young Lee[1,2,3], **Arijeet K. Gattu**[1,4], **João-Paulo G. Camporez**[1], **Shoichi Kanda**[1], **Blas Guigni**[1], **Mario Kahn**[1], **Dongyan Zhang**[1], **Thomas Galbo**[1], **Andreas L. Birkenfeld**[1,5], **Francois R. Jornayvaz**[1], **Michael J. Jurczak**[1], **Cheol Soo Choi**[1,3], **Zhen Yan**[6], **R. Sanders Williams**[7], **Gerald I. Shulman**[1,2,8], and **Varman T. Samuel**[1,4]

[1]Department of Internal Medicine, Yale University School of Medicine, New Haven, CT 06520, USA

[2]Howard Hughes Medical Institute, Yale University School of Medicine, New Haven, CT, USA

[3]Lee Gil Ya Cancer and Diabetes Institute, Gachon University of Medicine and Science, Incheon, Korea

[4]Veteran's Affairs Medical Center, West Haven, CT, USA

[5]Department of Endocrinology, Charite – University School of Medicine, Berlin, Germany

[6]Department of Medicine, University of Virginia, Charlottesville, VA, USA

[7]J. David Gladstone Institutes, San Francisco, CA, USA

[8]Department of Cellular & Molecular Physiology, Yale University School of Medicine, New Haven, CT

Abstract

Aims/hypothesis—Aerobic exercise increases muscle glucose and improves insulin action through numerous pathways, including activation of Ca2+/calmodulin-dependent protein kinases (CAMKs) and peroxisome proliferator γ coactivator 1α (PGC-1α). While overexpression of PGC-1α increases muscle mitochondrial content and oxidative type I fibres, it does not improve insulin action. Activation of CAMK4 also increases the content of type I muscle fibres, PGC-1α level and mitochondrial content. However, it remains unknown whether CAMK4 activation improves insulin action on glucose metabolism in vivo.

Methods—The effects of CAMK4 activation on skeletal muscle insulin action were quantified using transgenic mice with a truncated and constitutively active form of CAMK4 (CAMK4*) in

Corresponding author: Varman T. Samuel, Department of Internal Medicine, Yale University School of Medicine, New Haven, CT 06520, USA, varman.samuel@yale.edu.

Duality of interest

The authors declare that there is no duality of interest associated with this manuscript.

Contribution statement

HL, AKG, JGC, SK, BG, MK, DZ, TG, ALB, FRJ and MJJ perform experiments, analysed data and revised the manuscript; HL, CSC, ZY, RSW, GIS, VTS designed study and revised the manuscript; HL, CSC, GIS, VTS were responsible for the conception of the study and drafting the article. All authors approved the final version.

skeletal muscle. Tissue-specific insulin sensitivity was assessed in vivo using a hyperinsulinaemic–euglycaemic clamp and isotopic measurements of glucose metabolism.

Results—The rate of insulin-stimulated whole-body glucose uptake was increased by ~25% in CAMK4* mice, which was largely attributed to an increase of ~60% in the glucose uptake in the quadriceps, the largest hindlimb muscle. These mice had improvements in insulin signalling, as reflected by increased phosphorylation of Akt and its substrates and an increase in the level of GLUT4 protein. In addition, there were extramuscular effects: CAMK4* mice had improved hepatic and adipose insulin action. These pleiotropic effects were associated with increased levels of PGC-1α-related myokines in CAMK4* skeletal muscle.

Conclusions/interpretation—Activation of CAMK4 enhances mitochondrial biogenesis in skeletal muscle while also coordinating improvements in whole-body insulin-mediated glucose utilisation.

Keywords

Hyperinsulinaemic–euglycaemic clamp; Muscle insulin resistance; Myokines

Introduction

Skeletal muscle insulin resistance is a major factor in the pathogenesis of type 2 diabetes [1–4] and metabolic syndrome [5]. In many instances, skeletal muscle insulin resistance develops when an increase in intramyocellular diacyglycerol (DAG) activates novel protein kinase C (nPKC) isoforms, such as PKC-θ, which attenuate insulin signalling, decreasing insulin-stimulated muscle glucose transport. This mechanism has been associated with obesity as well as inherited and acquired (e.g. with ageing) reductions in mitochondrial oxidative capacity [6, 7].

Both muscle insulin action and mitochondrial function can be improved with aerobic exercise training [8–12]. These cellular effects of exercise are multifaceted and coordinated by elaborate networks of signalling proteins [13]. Among these are the Ca^{2+}/calmodulin-dependent protein kinases (CAMKs), a family of serine/threonine protein kinases that mediate a cellular response to intracellular Ca^{2+}. Exercise activates skeletal muscle CAMK activity and may coordinate the cellular changes of aerobic training [14–17]. Wu and colleagues created a novel transgenic mouse strain in which a truncated and constitutively active form of CAMK4 (CAMK4*) is expressed under the control of muscle creatine kinase [18]. Although CAMK2 is the main muscle isoform, CAMK4 shares common downstream targets, such as cAMP response element binding protein (CREB) [14, 19–22] and myocyte enhancer factor 2 (MEF2) [23]. Thus, CAMK4* mice serve as a model in which to explore the functional consequences of CAMK activation in skeletal muscle. CAMK4* mice exhibit transformation of fast-twitch skeletal muscle fibres (type II) to slow-twitch fibres (type I) [18, 24]. This is associated with increased mitochondrial biogenesis [18], possibly via increased CREB and MEF2-mediated transcription of the peroxisome proliferator-activated receptor γ coactivator 1α gene (*Ppargc1a*) [25]. PGC-1α mediates many musculoskeletal adaptations to exercise, including increased endurance [26], mitochondrial biogenesis [27] and enhanced lipid [28] and glucose uptake [29]. But mice with increased levels of PGC-1α

fed a high-fat diet are, paradoxically, prone to muscle steatosis and muscle insulin resistance [30]. Thus, while aerobic exercise clearly improves insulin action, increased levels of PGC-1α per se do not.

As exercise is also associated with CAMK activation, we hypothesised that muscle-specific activation of CAMK4 would increase insulin sensitivity in vivo. We assessed insulin sensitivity in wild-type (WT) and CAMK4* mice using the hyperinsulinaemic–euglycaemic clamp. We subsequently examined the potential cellular pathways through which muscle-specific activation of CAMK4 might improve insulin action.

Methods

Animals

The CAMK4* mice in the F3 hybrid C57BL/6 × SJL mice [18] were further back-crossed with female C57BL/6J mice over ten generations in the Yale animal facility. Male CAMK4* mice and age-matched littermate control male WT mice were studied at 6–7 months of age. Mice were individually housed under controlled temperature (23°C) and lighting (12 h light/12 h dark) conditions, with free access to water and ad libitum feeding with regular chow (RC, 2018S, Harlan Teklad, Madison, WI, USA). Body composition was assessed by ^{1}H-magnetic resonance spectroscopy (Bruker BioSpin, Billerica, MA, USA). The study was conducted at the National Institutes of Health (NIH)—Yale Mouse Metabolic Phenotyping Center. All procedures were approved by the Yale University Animal Care and Use Committee and followed the principles of animal care defined by NIH Office of Laboratory Animal Welfare.

Hyperinsulinaemic–euglycaemic clamp study

Catheterised animals were fasted overnight. Basal glucose turnover was assessed with an infusion of [3-^{3}H]glucose (HPLC purified; Perkin Elmer, Waltham, MA, USA) at a rate of 1.85 kBq/min for 2 h. The hyperinsulinaemic–euglycaemic clamp was conducted for 140 min with primed/continuous infusion of human insulin (~50 pmol kg^{-1} min^{-1} for 3 min prime, 20.8 pmol kg^{-1} min^{-1} continuous [Novo Nordisk, Plainsboro, NJ, USA]). During the clamp, a variable infusion of 20% (wt./vol.) dextrose was infused to maintain euglycaemia (~6.7 mmol/l). A bolus of 2-deoxy-D-[1-^{14}C]glucose (0.37 MBq per mouse, Perkin Elmer) was injected at 85 min to assess tissue-specific glucose uptake. On completion of the clamp, mice were killed with pentobarbital sodium injection (150 mg/kg) and all tissues were extracted and frozen immediately using liquid N_2. Tissues were stored at −80°C for subsequent analysis.

Plasma variables

Plasma glucose was analysed immediately after sampling using the glucose oxidase method and a YSI 2700 Biochemistry Analyzer (YSI Life sciences, Yellow Springs, OH. USA). Plasma insulin concentrations were measured by RIA using kits from Linco (St. Louis, MO,, USA). Plasma NEFA levels were determined using standard commercial kits according to the manufacturer's instructions (Wako Chemicals, Richmond, VA, USA).

Tissue lipid measurement

Tissue triacylglycerol was extracted using the method of Bligh and Dyer as described previously [7]. Intracellular DAG species were measured by liquid chromatography and tandem mass spectrometry as described previously [7]. Total DAG was expressed as the sum of individual species.

Quantitative RT-PCR analysis

WT and CAMK4* mice were fasted overnight prior to experiments. Total RNA was isolated using Trizol according to the manufacturer's instructions (Invitrogen, Carlsbad, CA, USA) from snap-frozen extensor digitorum longus (EDL) muscle tissue, normally a predominantly fast-twitch skeletal muscle, or epididymal white adipose tissue (WAT). Quantitative real-time PCR was then performed. Relative quantification of gene expression was performed using the standard curve method, and values were normalised to GAPDH expression. Data are normalised by the WT average. Primer sequences are shown in electronic supplementary material (ESM) Table 1.

Western blot analysis

Snap-frozen tissues from WT and CAMK4* mice were homogenised in lysis buffer containing 50 mmol/l HEPES (pH 7.0), 250 mmol/l NaCl, 0.1% NP40, 5 mmol/l EDTA, phosphatase inhibitor and complete proteinase inhibitor (Roche Molecular Biochemicals, Indianapolis, IN, USA). After centrifugation at 8,000 g for 15 min, supernatant fractions were resolved by SDS-PAGE, transferred to PVDF membranes and immunoblotted. For CAMK4 protein detection, nuclear protein was extracted from the frozen tissue (EDL) using a Dounce homogeniser and the NE-PER Nuclear and Cytoplasmic Extraction Kit (Pierce Biotechnology, Rockford, IL, USA). Immunoblots were quantified using ImageJ (NIH). The content of specific proteins was assessed by firstnormalising to GAPDH and then comparing each experimental sample with the average expression in the control (WT) group. The primary antibodies used in the current study were as follows: CAMK4 (Transduction Laboratories, Lexington, KY, USA); pAkt (Ser473), total Akt, p-AMP-activated protein kinase (AMPK) (Tyr172), total AMPK, pCREB (Ser133) and total CREB, pMEF2A (Thr312/Thr319), total MEF2A, 160 kDa substrate of the Akt serine/threonine kinase (AS160), pAS160 (Thr642), Akt1 substrate 1 (proline-rich) (PRAS40) and pPRAS40 (Thr246 (Cell Signaling, Danvers, MA, USA); PGC-1α, pACC2 on Ser219/Ser221, CD36 and GAPDH (Santa Cruz Biotechnology, Santa Cruz, CA, USA); GLUT4 C-terminus (gift of Dr J. S. Bogan [31]); PKC-θ, uncoupling protein 1 (mitochondrial, proton carrier) (UCP1) (Abcam, Cambridge, MA, USA).

Protein phosphatase type 2A activity assay

The protein phosphatase type 2A (PP2A) immunoprecipitation phosphatase assay kit purchased from Millipore (Temecula, CA, USA) was used to measure dephosphorylation of a phosphopeptide as an index of phosphatase activity. Briefly, the frozen tissues were lysed using the phosphatase extraction buffer specified by the assay kit, and the PP2A catalytic subunit (PP2A/C) was immunoprecipitated with anti-PP2A/C antibody supplied in the assay kit. Agarose-bound immune complexes were collected and resuspended in 80 μl serine/

threonine buffer with 750 μmol/l of phosphopeptide (obtained from the kit). The release of free phosphate was quantified after a 10 min incubation using Malachite Green. Results are expressed as fold change of PP2A activity compared with control.

Statistical analysis

Values are expressed as mean ± SEM. The significance of the differences in mean values between two groups was evaluated by two-tailed Student's *t* test. More than three groups were evaluated by ANOVA, followed by post hoc analysis using Bonferroni's multiple comparison test. A *p* value less than 0.05 was considered significant.

Results

Activation of CAMK4 increases PGC-1α-related mitochondrial genes and protein levels in fast-twitch skeletal muscle

The level of the truncated protein (Fig. 1a) and expression of the transgene (Fig. 1b) were increased in fast-twitch skeletal muscles (EDL and WQD) [18, 25]. This was associated with increases of ~40% in *Pgc-1α* (also known as *Ppargc1a*) mRNA and ~65% in myoglobin mRNA in the EDL muscle from CAMK4* mice (Fig. 1c). There was increased mRNA expression of key genes involved in mitochondrial function in EDL muscle from CAMK4* mice: carnitine palmitoyltransferase 1 (*Cpt1*), NADH-ubiquinone oxidoreductase 75 kDa subunit (*Ndufs1*), cytochrome oxidase subunit V (*Cox5b*) and ATP synthase β subunit (*Atp5b*) were all significantly increased (Fig. 1c). These data are consistent with the previously reported phenotype showing a fibre-type switch phenotype in CAMK4* transgenic mice producing the truncated form of CAMK4 in fast-twitch muscles [18].

CAMK4 increases PGC-1α expression via CREB activation [25]. We compared the protein level of PGC-1α and related protein phosphorylation of CREB in CAMK4* muscle with that in WT muscle (Fig. 1d). Both phosphorylation of CREB (Ser133) and PGC-1α level were significantly increased in CAMK4* muscle. The level of the mitochondrial membrane protein voltage-dependent ion channel (VDAC) was also increased by ~61% in WQD fast-twitch skeletal muscle (Fig. 1d). These data clearly show that CAMK4 activation increases PGC-1α expression associated with CREB phosphorylation, which results in significant changes in the expression of genes that increase mitochondrial biogenesis and is characterised by a conversion from type II to type I muscle fibres.

Activation of CAMK4 in skeletal muscle improves insulin action

To assess tissue-specific changes in insulin action, we performed hyperinsulinaemic–euglycaemic clamp studies in 6-month-old male mice fed a regular chow diet. Body weight, fat mass and lean body mass measured by H^1-magnetic resonance spectroscopy were similar between CAMK4* and WT mice (Table 1). Fasting plasma glucose concentrations were similar between the two groups, but fasting plasma insulin concentrations were decreased in CAMK4* mice (Table 1). During the hyperinsulinaemic–euglycaemic period, plasma glucose and insulin concentrations were matched between the two groups (Table 1 and Fig. 2a), but the glucose infusion rates required to maintain euglycaemia (~6.6 mmol/l) in

CAMK4* mice were ~40% higher than those for WT mice (Fig. 2a), indicating an increase in whole-body insulin sensitivity of CAMK4* mice.

Insulin-stimulated whole-body glucose uptake and endogenous glucose production (EGP) were quantified during the hyperinsulinaemic–euglycaemic clamp using radiolabelled glucose. Insulin-stimulated peripheral glucose uptake was significantly increased by ~25% in CAMK4* mice compared with WT mice (Fig. 2b). Tissue 2-deoxy-D-[1-^{14}C]glucose uptake identified which tissues contributed to this increase in whole-body insulin-mediated glucose uptake. The increase in whole-body insulin-stimulated glucose uptake could be largely attributed to an increase in fast-twitch muscle glucose uptake, the predominant fibre type in mice [32]. There was a ~60% increase in WQD (Fig. 3a), the largest skeletal muscle in the hindlimb and comprising predominantly type II fast-twitch muscle fibres [33]. Insulin-stimulated 2-deoxy-D-[1-^{14}C]glucose uptake was not significantly different in heart (Fig. 3c) or mixed-type muscle (gastrocnemius muscle) (Fig. 3b).

The improvements in muscle insulin sensitivity were associated with improvements in insulin signalling. Insulin-stimulated Akt phosphorylation (Ser473) was significantly increased in both fast-twitch muscle (Fig. 4a) and liver (Fig. 4b) of CAMK4* mice compared with WT mice. Furthermore, phosphorylation of AS160 [34] was increased in fast-twitch muscle of CAMK4* mice (Fig. 4c). Thus CAMK4* expression improves insulin-stimulated muscle glucose uptake.

Muscle-specific CAMK4* production was associated with extramuscular improvements in insulin action. Although basal rates of EGP were not different, insulin suppression of EGP was nearly 100% in CAMK4* mice compared with a 41% suppression in WT mice (Fig. 2c), suggesting increased hepatic insulin sensitivity. There were also improvements in adipose insulin sensitivity as seen with the ~40% increase in 2-deoxy-D-[1-^{14}C]glucose uptake in adipose tissue (Fig. 3d). In contrast, suppression of lipolysis (as reflected by plasma NEFA concentration during the clamp) was not altered (Table 1). Thus, muscle-specific CAMK4* expression also improves hepatic and adipose insulin responsiveness, which may contribute to the whole-body improvements in insulin-stimulated glucose metabolism.

Activation of CAMK4 in skeletal muscle increases expression of myokine mRNAs

Recent studies have implicated the PGC-1α-regulated myokines as the mediators of the extramuscular improvements in whole-body metabolism with exercise [35–38]. To determine if these myokines explain the extramuscular effects seen with CAMK4* in, specifically, fast-twitch muscles, we measured the gene expression of key myokines (FNDC5, *Vegf-β* [also known as *Vegfb*], *Il15*, *Il6* and *Fgf21*) in skeletal muscle. The expression of FNDC5, *Vegfb* and *Il15* mRNAs was significantly increased in the fast-twitch muscle from CAMK4* mice, whereas there were no significant differences in *Il6* and *Fgf21* gene expression between genotypes (Fig. 5a). These data are consistent with previous findings that identified FNDC5, vascular endothelial growth factor B (VEGF-β) and IL-15 as PGC-1α-related myokines [37]. In the present study, the increased myokine expression was associated with an increase in the WAT expression of *Ucp1* and *Prdm16* mRNA (Fig. 5b) as well as an increase in UCP1 protein level (Fig. 5c) in CAMK4* mice compared with WT mice. In these chow-fed mice, these changes did not alter body weight or adiposity.

These data suggest that activation of CAMK4 in skeletal muscle may enhance whole-body insulin sensitivity via increases in myokine expression.

Activation of CAMK4 in skeletal muscle maintains normal lipid content

PGC-1α can activate peroxisome proliferator-activated receptor γ (PPARγ), which may alter the production of key proteins in lipid metabolism [39]. But increases in muscle lipid content, specifically DAG, could activate PKC-θ by promoting membrane translocation, which may then impair insulin signalling [7, 40–42]. The mRNA and protein expression of CD36 molecule (thrombospondin receptor) (CD36), a key fatty acid transporter, and diacylglycerol O-acyltransferase 1 (DGAT1), a key rate-controlling enzyme for triacylglycerol re-esterification, were increased in fast-twitch muscle from CAMK4* mice (Fig. 6d, e). Despite this, there were no differences in intramyocellular DAG (Fig. 6b) or triacylglycerol content (Fig. 6a). Accordingly, translocation of PKC-θ, a DAG-responsive nPKC, was similar (Fig. 6c). Thus, alterations in the PKC-θ cannot account for the improvements in muscle insulin signalling.

To assess other mechanisms that may regulate Akt2 activity, we measured PP2A activity in fast-twitch skeletal muscle. PP2A has a binding site on the N-terminus of CAMK4 (the active form has an N-terminus) [19, 43] and can inhibit Akt activity [44]. As expected, muscle PP2A activity was significantly increased in CAMK4* mice in the basal fasted state and decreased to WT levels at the end of the hyperinsulinaemic clamp study (Fig. 6f). It may be possible that PP2A activity is tonically increased in CAMK4* mice and that the decrease following insulin stimulation permits the increase in Akt2 phosphorylation.

MEF2A, AMPK and GLUT4

CAMK4* can also increase the activity of MEF2A, a transcription factor that, in turn, may regulate GLUT4 expression [16]. MEF2A activation was assessed by quantifying phosphorylation on Thr312 and Thr319 [45]. We observed increased phosphorylation of MEF2A (Fig. 7a) in the fast-twitch muscle obtained at the end of the hyperinsulinaemic–euglycaemic clamp. This was associated with increased GLUT4 protein levels (Fig. 7b) and a trend to increased *Glut4* mRNA expression in the fast-twitch muscle from the CAMK4* mice compared with WT muscle (Fig. 7c). In contrast, GLUT4 expression was not different in the gastrocnemius, a muscle that does not have increased levels of CAMK* (data not shown). There were also significant increases in AMPK phosphorylation and ACC2 phosphorylation in the skeletal muscle of CAMK* mice (Fig. 7d); AMPK may also regulate GLUT4 expression [46]. Thus, CAMK* overexpression appears to promote activation of MEF2A and AMPK, which, in turn, may account for the increase in GLUT4 expression and increased capacity for insulin-stimulated skeletal muscle glucose uptake.

Discussion

Aerobic exercise improves mitochondrial function and could correct an underlying cause of insulin resistance [47]. But incorporating aerobic exercise into a sedentary lifestyle is a challenge for many patients, especially when their condition is compounded by comorbid

disease. Thus, efforts have focused on trying to recapitulate the cellular and molecular changes induced by aerobic exercise.

CAMKs are key components of the signalling network activated by aerobic exercise. Here, we found that activation of CAMK4 improved whole-body insulin-stimulated glucose uptake. The ~25% increase in whole-body glucose turnover is mainly accounted by ~60% increased glucose specifically in fast-twitch muscle, the predominant fibre type in mice [32, 33]. Activation of CAMK4 was associated with increased expression of PGC-1α and key mitochondrial proteins, consistent with previous observations of increased mitochondrial biogenesis in CAMK4* mice. However, the phenotype in CAMK4* mice extends beyond the increase in PGC-1α level.

The conclusion is supported by previous findings that PGC-1α transgenic mice had increased mitochondrial content but were prone to muscle lipid accumulation and muscle insulin resistance when fed a high-fat diet [30]. This discordance may be due to an increase in muscle fatty acid transport and synthesis that led to muscle lipid accumulation despite the augmented oxidative capacity [39]. Recently, Summermatter et al reported that PGC-1α transgenic animals fed even a regular chow diet had a decrease in glucose tolerance and muscle glucose uptake associated with an increase in some muscle lipid metabolites, including DAG, acyl-carnitines and sphingosine [48]. Thus, while expression of PGC-1α is sufficient to promote mitochondrial biogenesis, it does not necessarily improve insulin action.

In contrast, CAMK4* mice fed a chow diet did not have changes in muscle triacylglycerol or DAG content. This difference could be due to the degree of PGC-1α expression. CAMK4* increased PGC-1α expression by ~50% compared with a two- to fourfold increase with the PGC-1α transgenic mice [30]. It is also possible that the effects seen in the CAMK4* mice may be due to a broader coordinated set of changes that may mimic the multiple effects of exercise. This was also seen by Summermatter and colleagues when they subjected WT and PGC-1α mice to aerobic conditioning. The transgenic mice surpassed the WT mice, with greater improvements in endurance and glucose tolerance [48]. Thus, while activation of PGC-1α may enhance the response to exercise, activation of CAMK may better mimic the effects of exercise on insulin action.

CAMK4 activation was associated with increased expression of several key metabolic regulators: CREB (Fig. 1d) AMPK and MEF2A (Fig. 7a). MEF2A is a key regulator of *Glut4* gene expression [49]. Both AMPK [50] and CAMK4 [51] have been shown to phosphorylate histone deacetylase 5 (HDAC5), a transcriptional repressor that prevents cofactors from binding to MEF2A. When phosphorylated, HDAC5 dissociates from MEF2A, allowing it to bind co-activators, including PGC-1α [51]. The increase in muscle GLUT4 expression in CAMK4* mice is consistent with prior in vitro studies demonstrating that CAMK4 activates MEF2A in cardiac muscle [52]. Previous studies have demonstrated that overexpression of GLUT4 increases insulin-stimulated muscle glucose uptake [53]. Although the improvements in muscle glucose uptake in CAMK4* mice are modest compared with the GLUT4 transgenic mice, this is consistent with the lesser degree of GLUT4 overexpression. Thus, in CAMK4* mice, activation of MEF2A may increase

expression of GLUT4 and enhance insulin-stimulated muscle glucose uptake. By comparison, *Glut4* mRNA expression and glucose uptake are decreased in untrained PGC-1α transgenic mice [48].

In addition, the insulin-signalling cascade was more active in CAMK4* mice. We observed an increase in insulin-stimulated phosphorylation of Akt (Ser473) in skeletal muscle as well as phosphorylation of downstream targets. The exact mechanism is unclear. Akt is not a direct substrate for CAMK4. Further, while decreases in muscle lipid content are associated with improvements in insulin signalling in some models, there were no differences in muscle lipid content between the chow-fed WT and CAMK4* mice. One clue to a possible mechanism is the observation is that PP2A activity is altered in CAMK4* mice. Although activity was higher under basal conditions, it decreased to WT levels with insulin. PP2A activity was not changed with insulin in the WT animals. Thus, the ability to decrease PP2A activity would allow for the increase in Akt2 phosphorylation. Thus, an improvement in insulin signalling and an increase in GLUT4 content may both contribute to the increase in insulin-stimulated muscle glucose uptake.

Additionally, the improvements in hepatic insulin sensitivity were associated with an increase in insulin-stimulated hepatic Akt phosphorylation relative to basal phosphorylation. These data suggest that CAMK4* expression in skeletal muscle may lead to systemic improvements in insulin sensitivity. The expression of *Fndc5*, *Vegfb* and *Il15* was increased in the CAMK4* mice. These myokines have been implicated in mediating the extramuscular improvements in whole-body metabolism with exercise [35–38]. The effects of these myokines may be subtle. The increased expression of myokines was associated with the enhanced UCP1 expression in adipose tissue, an increase in adipose tissue glucose uptake and improvements in hepatic insulin sensitivity. However, there were no measurable differences in body mass, adiposity or tissue lipid content in these regular-chow-fed animals.

In conclusion, the expression of an active form of CAMK4 in muscle improved insulin-stimulated muscle glucose uptake, with increases in GLUT4 content and improvements in insulin signalling. Moreover, CAMK4 activation also improved hepatic and adipose insulin action, possibly via increases in myokines released from the skeletal muscle. Taken together, these results suggest skeletal CAMK activation may recapitulate the effects of exercise, enhancing muscle insulin action while also coordinating improvements in whole-body insulin action.

Supplementary Material

Refer to Web version on PubMed Central for supplementary material.

Acknowledgments

The authors would like to thank D. W. Frederick, Y. Kosover, I. Moore and A. Groszmann (Yale University School of Medicine, New Haven, CT, USA) for expert technical assistance with the studies.

Funding

This work was supported by grants from the US Public Health Service (R01 DK-40936, P30 DK-45735, U24 DK-059635) and a VA Merit Award (VTS). ALB was supported by a grant from the German Research Foundation (DFG, BI1292/4-1). ZY was supported by NIH grant AR050429.

Abbreviations

AMPK	AMP-activated protein kinase
AS160	160 kDa substrate of the Akt serine/threonine kinase
CAMK	Ca^{2+}/calmodulin-dependent protein kinase
CAMK4*	Truncated and constitutively active form of CAMK
CREB	cAMP response element binding protein
DAG	Diacylglycerol
EGP	Endogenous glucose production
EDL	Extensor digitorum longus
HDAC5	Histone deacetylase 5
MEF2	Myocyte enhancer factor 2
NIH	National Institutes of Health
nPKC	Novel protein kinase C
PGC-1α	Peroxisome proliferator-activated receptor γ coactivator 1α
PP2A	Protein phosphatase type 2A
PP2A/C	Protein phosphatase type 2A catalytic subunit
PRAS40	Akt1 substrate 1 (proline-rich)
UCP1	Uncoupling protein 1 (mitochondrial, proton carrier)
VDAC	Voltage-dependent ion channel
WAT	White adipose tissue
WQD	White quadriceps

References

1. Shulman GI, Rothman DL, Jue T, Stein P, DeFronzo RA, Shulman RG. Quantitation of muscle glycogen synthesis in normal subjects and subjects with non-insulin-dependent diabetes by 13C nuclear magnetic resonance spectroscopy. N Engl J Med. 1990; 322:223–228. [PubMed: 2403659]
2. Cline GW, Petersen KF, Krssak M, et al. Impaired glucose transport as a cause of decreased insulin-stimulated muscle glycogen synthesis in type 2 diabetes. N Engl J Med. 1999; 341:240–246. [PubMed: 10413736]
3. Rothman DL, Magnusson I, Cline G, et al. Decreased muscle glucose transport/phosphorylation is an early defect in the pathogenesis of non-insulin-dependent diabetes mellitus. Proceedings of the

National Academy of Sciences of the United States of America. 1995; 92:983–987. [PubMed: 7862678]

4. DeFronzo RA. Insulin resistance, lipotoxicity, type 2 diabetes and atherosclerosis: the missing links. The Claude Bernard Lecture 2009. Diabetologia. 2010; 53:1270–1287. [PubMed: 20361178]
5. DeFronzo RA. Insulin resistance: a multifaceted syndrome responsible for NIDDM, obesity, hypertension, dyslipidaemia and atherosclerosis. The Netherlands Journal of Medicine. 1997; 50:191–197. [PubMed: 9175399]
6. Petersen KF, Dufour S, Befroy D, Garcia R, Shulman GI. Impaired mitochondrial activity in the insulin-resistant offspring of patients with type 2 diabetes. N Engl J Med. 2004; 350:664–671. [PubMed: 14960743]
7. Lee HY, Choi CS, Birkenfeld AL, et al. Targeted expression of catalase to mitochondria prevents age-associated reductions in mitochondrial function and insulin resistance. Cell Metab. 2010; 12:668–674. [PubMed: 21109199]
8. Rabol R, Petersen KF, Dufour S, Flannery C, Shulman GI. Reversal of muscle insulin resistance with exercise reduces postprandial hepatic de novo lipogenesis in insulin resistant individuals. Proceedings of the National Academy of Sciences of the United States of America. 2011; 108:13705–13709. [PubMed: 21808028]
9. Ren JM, Semenkovich CF, Gulve EA, Gao J, Holloszy JO. Exercise induces rapid increases in GLUT4 expression, glucose transport capacity, and insulin-stimulated glycogen storage in muscle. The Journal of Biological Chemistry. 1994; 269:14396–14401. [PubMed: 8182045]
10. Phielix E, Meex R, Moonen-Kornips E, Hesselink MK, Schrauwen P. Exercise training increases mitochondrial content and ex vivo mitochondrial function similarly in patients with type 2 diabetes and in control individuals. Diabetologia. 2010; 53:1714–1721. [PubMed: 20422397]
11. Holloszy JO. Biochemical adaptations in muscle. Effects of exercise on mitochondrial oxygen uptake and respiratory enzyme activity in skeletal muscle. The Journal of Biological Chemistry. 1967; 242:2278–2282. [PubMed: 4290225]
12. Perseghin G, Price TB, Petersen KF, et al. Increased glucose transport-phosphorylation and muscle glycogen synthesis after exercise training in insulin-resistant subjects. N Engl J Med. 1996; 335:1357–1362. [PubMed: 8857019]
13. Roden M. Exercise in type 2 diabetes: to resist or to endure? Diabetologia. 2012; 55:1235–1239. [PubMed: 22391950]
14. Rose AJ, Kiens B, Richter EA. Ca2+-calmodulin-dependent protein kinase expression and signalling in skeletal muscle during exercise. The Journal of Physiology. 2006; 574:889–903. [PubMed: 16690701]
15. Egan B, Carson BP, Garcia-Roves PM, et al. Exercise intensity-dependent regulation of peroxisome proliferator-activated receptor coactivator-1 mRNA abundance is associated with differential activation of upstream signalling kinases in human skeletal muscle. The Journal of Physiology. 2010; 588:1779–1790. [PubMed: 20308248]
16. Smith JA, Collins M, Grobler LA, Magee CJ, Ojuka EO. Exercise and CaMK activation both increase the binding of MEF2A to the Glut4 promoter in skeletal muscle in vivo. American Journal of Physiology Endocrinology and Metabolism. 2007; 292:E413–420. [PubMed: 16985263]
17. Serpiello FR, McKenna MJ, Stepto NK, Bishop DJ, Aughey RJ. Performance and physiological responses to repeated-sprint exercise: a novel multiple-set approach. European Journal of Applied Physiology. 2011; 111:669–678. [PubMed: 20957389]
18. Wu H, Kanatous SB, Thurmond FA, et al. Regulation of mitochondrial biogenesis in skeletal muscle by CaMK. Science. 2002; 296:349–352. [PubMed: 11951046]
19. Westphal RS, Anderson KA, Means AR, Wadzinski BE. A signaling complex of Ca2+-calmodulin-dependent protein kinase IV and protein phosphatase 2A. Science. 1998; 280:1258–1261. [PubMed: 9596578]
20. Wu JY, Ribar TJ, Cummings DE, Burton KA, McKnight GS, Means AR. Spermiogenesis and exchange of basic nuclear proteins are impaired in male germ cells lacking Camk4. Nature Genetics. 2000; 25:448–452. [PubMed: 10932193]
21. Sato K, Suematsu A, Nakashima T, et al. Regulation of osteoclast differentiation and function by the CaMK-CREB pathway. Nature Medicine. 2006; 12:1410–1416.

22. Wright DC, Hucker KA, Holloszy JO, Han DH. Ca2+ and AMPK both mediate stimulation of glucose transport by muscle contractions. Diabetes. 2004; 53:330–335. [PubMed: 14747282]
23. Blaeser F, Ho N, Prywes R, Chatila TA. Ca(2+)-dependent gene expression mediated by MEF2 transcription factors. The Journal of Biological Chemistry. 2000; 275:197–209. [PubMed: 10617605]
24. Lin J, Wu H, Tarr PT, et al. Transcriptional co-activator PGC-1 alpha drives the formation of slow-twitch muscle fibres. Nature. 2002; 418:797–801. [PubMed: 12181572]
25. Handschin C, Rhee J, Lin J, Tarr PT, Spiegelman BM. An autoregulatory loop controls peroxisome proliferator-activated receptor gamma coactivator 1alpha expression in muscle. Proceedings of the National Academy of Sciences of the United States of America. 2003; 100:7111–7116. [PubMed: 12764228]
26. Calvo JA, Daniels TG, Wang X, et al. Muscle-specific expression of PPARgamma coactivator-1alpha improves exercise performance and increases peak oxygen uptake. J Appl Physiol. 2008; 104:1304–1312. [PubMed: 18239076]
27. Wu Z, Puigserver P, Andersson U, et al. Mechanisms controlling mitochondrial biogenesis and respiration through the thermogenic coactivator PGC-1. Cell. 1999; 98:115–124. [PubMed: 10412986]
28. Summermatter S, Baum O, Santos G, Hoppeler H, Handschin C. Peroxisome proliferator-activated receptor γ coactivator 1α (PGC-1α) promotes skeletal muscle lipid refueling in vivo by activating de novo lipogenesis and the pentose phosphate pathway. The Journal of Biological Chemistry. 2010; 285:32793–32800. [PubMed: 20716531]
29. Wende AR, Schaeffer PJ, Parker GJ, et al. A role for the transcriptional coactivator PGC-1alpha in muscle refueling. The Journal of Biological Chemistry. 2007; 282:36642–36651. [PubMed: 17932032]
30. Choi CS, Befroy DE, Codella R, et al. Paradoxical effects of increased expression of PGC-1alpha on muscle mitochondrial function and insulin-stimulated muscle glucose metabolism. Proceedings of the National Academy of Sciences of the United States of America. 2008; 105:19926–19931. [PubMed: 19066218]
31. Bogan JS, Hendon N, McKee AE, Tsao TS, Lodish HF. Functional cloning of TUG as a regulator of GLUT4 glucose transporter trafficking. Nature. 2003; 425:727–733. [PubMed: 14562105]
32. Bloemberg D, Quadrilatero J. Rapid determination of myosin heavy chain expression in rat, mouse, and human skeletal muscle using multicolor immunofluorescence analysis. PloS One. 2012; 7:e35273. [PubMed: 22530000]
33. Carlson CJ, Booth FW, Gordon SE. Skeletal muscle myostatin mRNA expression is fiber-type specific and increases during hindlimb unloading. The American Journal of Physiology. 1999; 277:R601–606. [PubMed: 10444569]
34. Sano H, Kane S, Sano E, et al. Insulin-stimulated phosphorylation of a Rab GTPase-activating protein regulates GLUT4 translocation. The Journal of Biological Chemistry. 2003; 278:14599–14602. [PubMed: 12637568]
35. Handschin C, Spiegelman BM. The role of exercise and PGC1alpha in inflammation and chronic disease. Nature. 2008; 454:463–469. [PubMed: 18650917]
36. Pedersen BK, Akerstrom TC, Nielsen AR, Fischer CP. Role of myokines in exercise and metabolism. J Appl Physiol. 2007; 103:1093–1098. [PubMed: 17347387]
37. Bostrom P, Wu J, Jedrychowski MP, et al. A PGC1-alpha-dependent myokine that drives brown-fat-like development of white fat and thermogenesis. Nature. 2012; 481:463–468. [PubMed: 22237023]
38. Nielsen AR, Mounier R, Plomgaard P, et al. Expression of interleukin-15 in human skeletal muscle effect of exercise and muscle fibre type composition. The Journal of Physiology. 2007; 584:305–312. [PubMed: 17690139]
39. Teboul L, Febbraio M, Gaillard D, Amri EZ, Silverstein R, Grimaldi PA. Structural and functional characterization of the mouse fatty acid translocase promoter: activation during adipose differentiation. The Biochemical Journal. 2001; 360:305–312. [PubMed: 11716758]
40. Petersen KF, Befroy D, Dufour S, et al. Mitochondrial dysfunction in the elderly: possible role in insulin resistance. Science. 2003; 300:1140–1142. [PubMed: 12750520]

41. Shulman GI. Cellular mechanisms of insulin resistance. The Journal of Clinical Investigation. 2000; 106:171–176. [PubMed: 10903330]
42. Griffin ME, Marcucci MJ, Cline GW, et al. Free fatty acid-induced insulin resistance is associated with activation of protein kinase C theta and alterations in the insulin signaling cascade. Diabetes. 1999; 48:1270–1274. [PubMed: 10342815]
43. Anderson KA, Noeldner PK, Reece K, Wadzinski BE, Means AR. Regulation and function of the calcium/calmodulin-dependent protein kinase IV/protein serine/threonine phosphatase 2A signaling complex. The Journal of Biological Chemistry. 2004; 279:31708–31716. [PubMed: 15143065]
44. Ugi S, Imamura T, Maegawa H, et al. Protein phosphatase 2A negatively regulates insulin's metabolic signaling pathway by inhibiting Akt (protein kinase B) activity in 3T3-L1 adipocytes. Molecular and Cellular Biology. 2004; 24:8778–8789. [PubMed: 15367694]
45. Zhao M, New L, Kravchenko VV, et al. Regulation of the MEF2 family of transcription factors by p38. Molecular and Cellular Biology. 1999; 19:21–30. [PubMed: 9858528]
46. Holmes BF, Kurth-Kraczek EJ, Winder WW. Chronic activation of 5′-AMP-activated protein kinase increases GLUT-4, hexokinase, and glycogen in muscle. J Appl Physiol. 1999; 87:1990–1995. [PubMed: 10562646]
47. Carey AL, Kingwell BA. Novel pharmacological approaches to combat obesity and insulin resistance: targeting skeletal muscle with 'exercise mimetics'. Diabetologia. 2009; 52:2015–2026. [PubMed: 19547950]
48. Summermatter S, Shui G, Maag D, Santos G, Wenk MR, Handschin C. PGC-1alpha improves glucose homeostasis in skeletal muscle in an activity-dependent manner. Diabetes. 2013; 62:85–95. [PubMed: 23086035]
49. Thai MV, Guruswamy S, Cao KT, Pessin JE, Olson AL. Myocyte enhancer factor 2 (MEF2)-binding site is required for GLUT4 gene expression in transgenic mice. Regulation of MEF2 DNA binding activity in insulin-deficient diabetes. The Journal of Biological Chemistry. 1998; 273:14285–14292. [PubMed: 9603935]
50. McGee SL, Howlett KF, Starkie RL, Cameron-Smith D, Kemp BE, Hargreaves M. Exercise increases nuclear AMPK alpha2 in human skeletal muscle. Diabetes. 2003; 52:926–928. [PubMed: 12663462]
51. McKinsey TA, Zhang CL, Lu J, Olson EN. Signal-dependent nuclear export of a histone deacetylase regulates muscle differentiation. Nature. 2000; 408:106–111. [PubMed: 11081517]
52. Passier R, Zeng H, Frey N, et al. CaM kinase signaling induces cardiac hypertrophy and activates the MEF2 transcription factor in vivo. The Journal of Clinical Investigation. 2000; 105:1395–1406. [PubMed: 10811847]
53. Ren JM, Marshall BA, Mueckler MM, McCaleb M, Amatruda JM, Shulman GI. Overexpression of Glut4 protein in muscle increases basal and insulin-stimulated whole body glucose disposal in conscious mice. The Journal of Clinical Investigation. 1995; 95:429–432. [PubMed: 7814644]

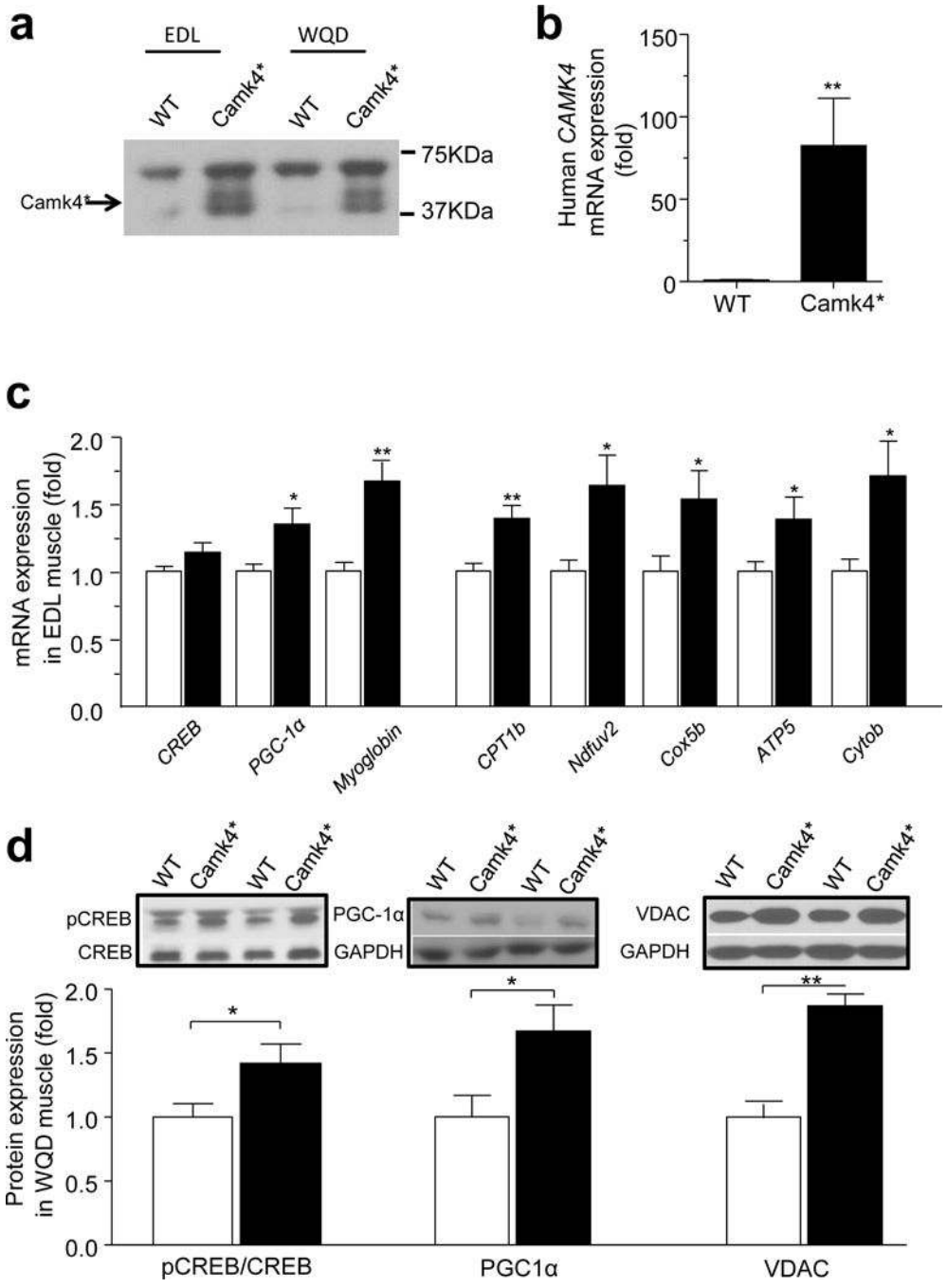

Fig. 1.

Mitochondrial genes and protein expression are increased in fast-twitch skeletal muscle from CAMK4* mice. (**a**) Truncated CAMK4 protein in the nuclear fraction of EDL and WQD muscle. (**b**) Human *CAMK4* mRNA expression in EDL muscle (n=6). (**c**) Expression of mRNAs for CAMK4-related genes involved in mitochondrial biogenesis (n=6). (**d**) Representative images and quantification of results for protein levels of PGC-1α, CREB and VDAC in WQD muscle from WT or CAMK4* mice (n=6–7). *p<0.05 and **p<0.01 by unpaired Student's t test compared with WT. White bars, WT; black bars, CAMK4*

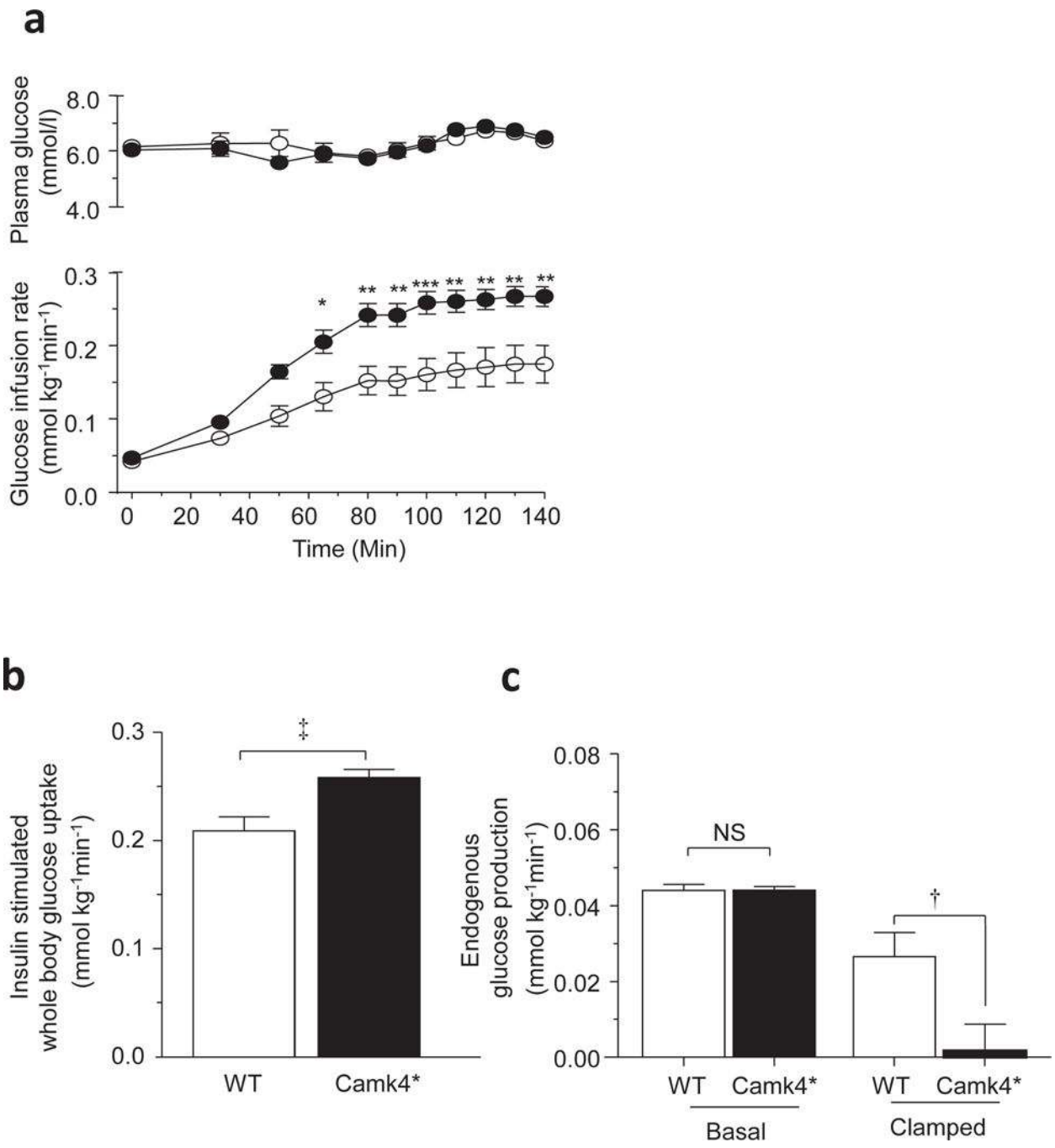

Fig. 2.

Insulin sensitivity, whole-body and tissue-specific glucose disposal in CAMK4* and WT mice during the hyperinsulinaemic–euglycaemic clamp. (**a**) Glucose infusion rate and plasma glucose concentration during the clamp (n=8). (**b**) Insulin-stimulated whole-body glucose uptake during the clamp (n=8). (**c**) EGP during the clamp (n=8). White circles, WT; black circles, CAMK4*. *p<0.05, **p<0.01 and ***p<0.001 by two-way ANOVA with post hoc analysis. $^{\dagger}p$<0.05 and $^{\dagger\dagger}p$<0.01 by unpaired Student's t test

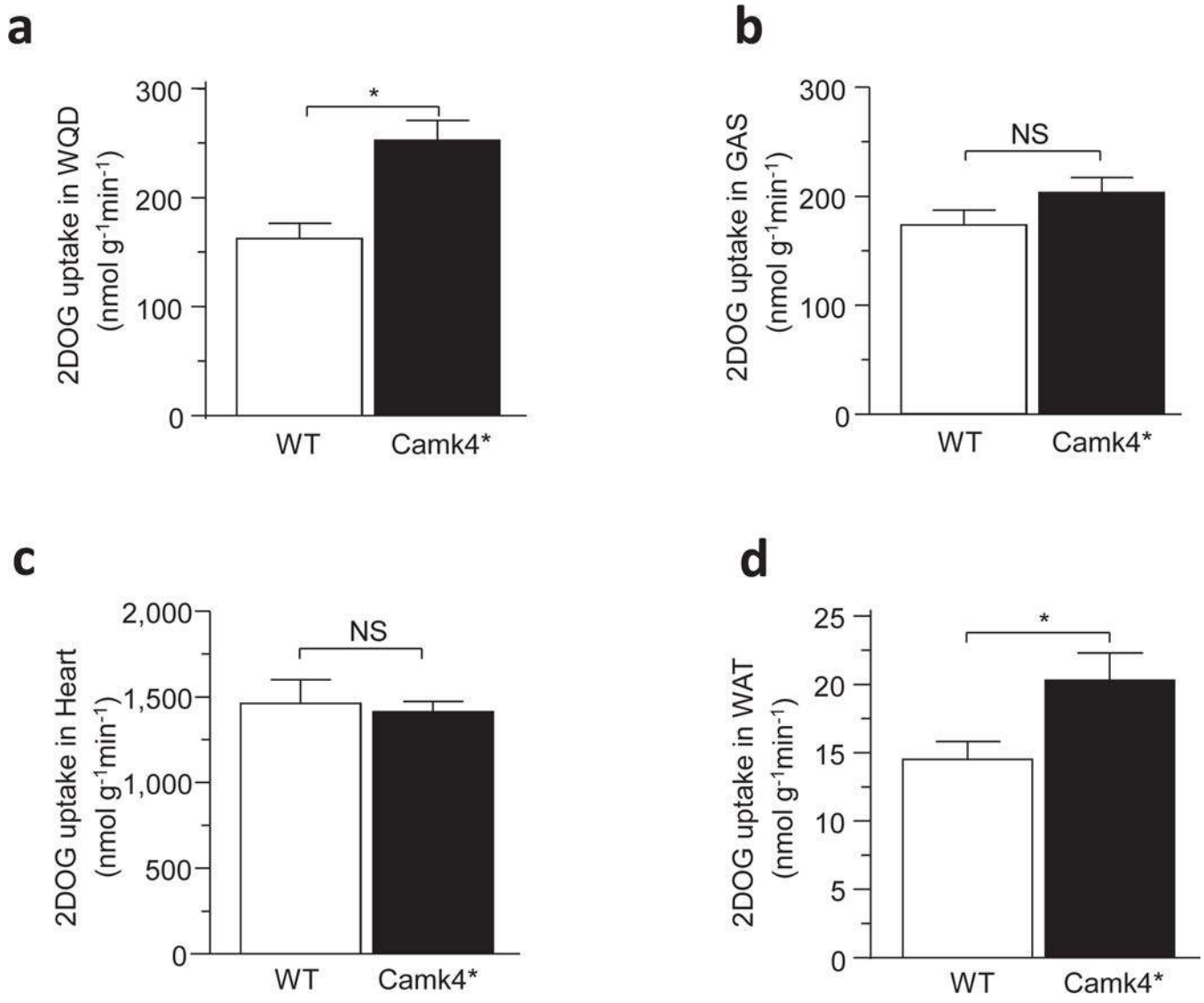

Fig. 3.

Insulin-stimulated 2-deoxy-D-[1-^{14}C]glucose uptake in various tissues during the steady state: WQD (**a**), GAS (**b**), heart (**c**) and WAT (**d**); (n=8). All data are mean ± SEM. *p<0.05 by unpaired Student's t test. 2DOG, 2-deoxy-D-[1-^{14}C]glucose; Gas., gastrocnemius

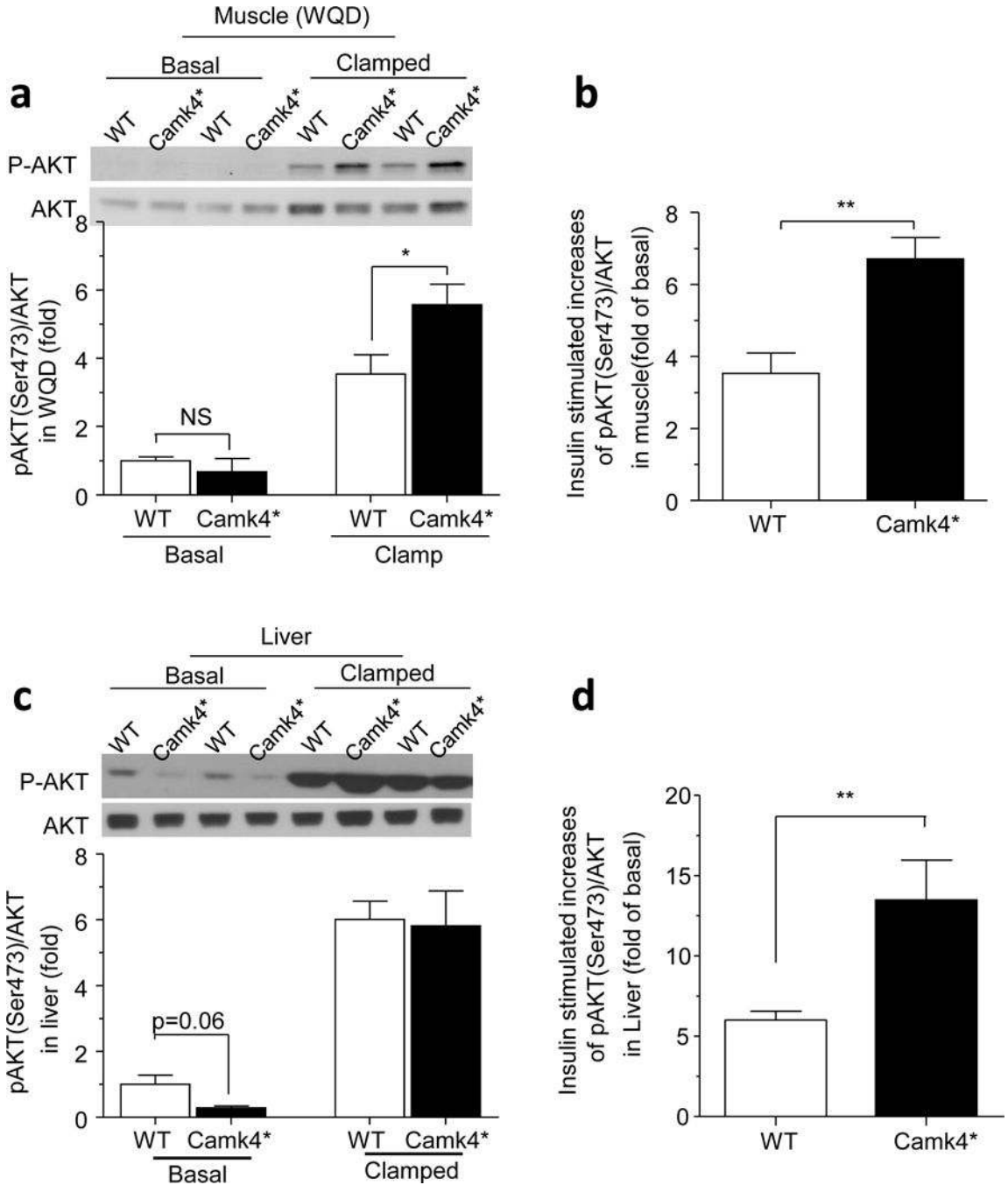

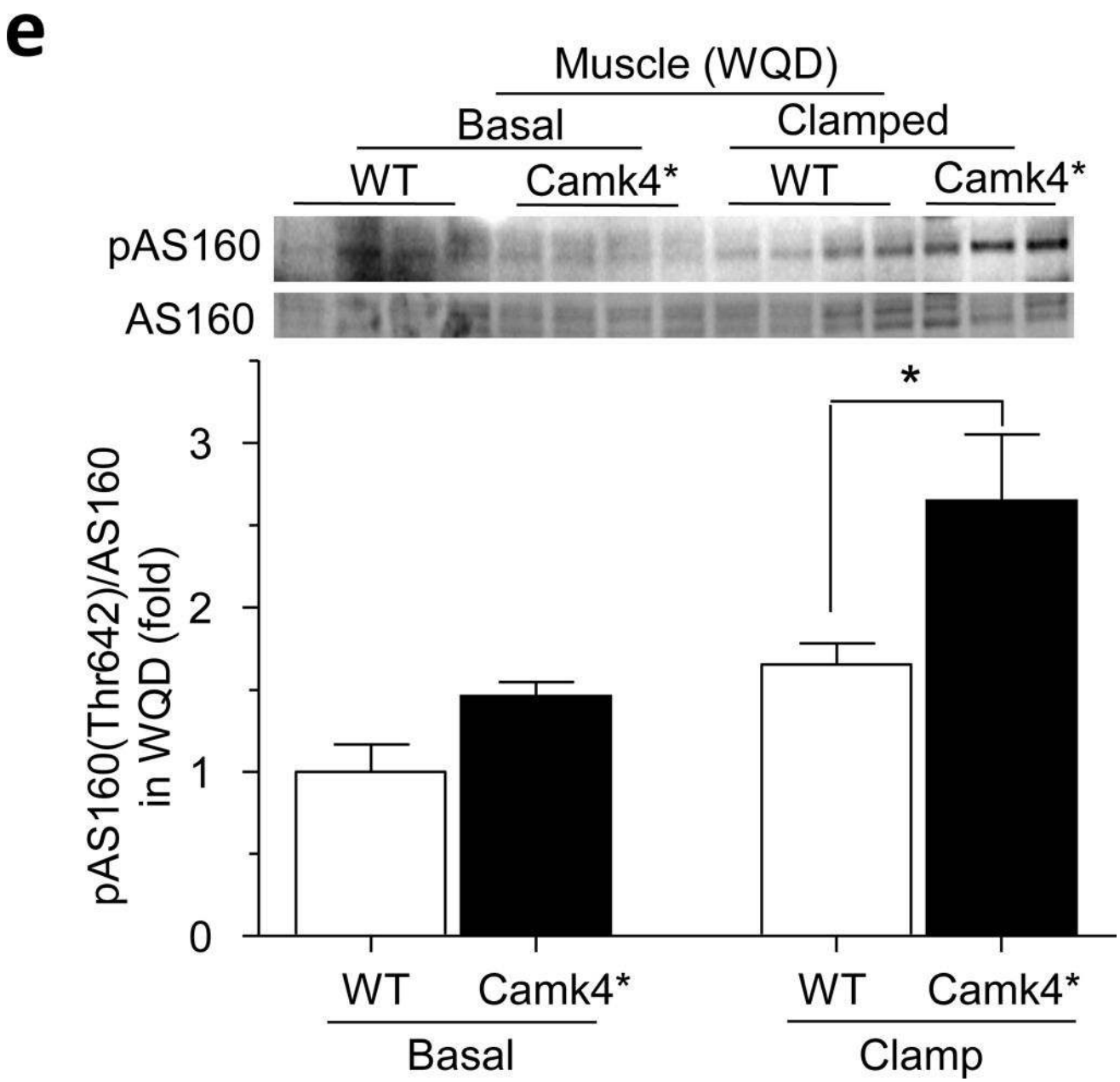

Fig. 4.

Insulin-responsive phosphorylation of Akt (Ser473) in skeletal muscle and liver. Basal samples were taken from animals after a 16 h overnight fast (n=6). Insulin-stimulated samples were taken from the animals after the hyperinsulinaemic–euglycaemic clamp study (n=8). Representative images and quantification of results for Akt phosphorylation on Ser473 in WQD muscle (**a**, **b**) and liver (**c**, **d**). The insulin-stimulated increases in Akt phosphorylation are expressed as fold changes from mean basal expression of each group (**b**, **d**). *p<0.05 and **p ≤0.01 by unpaired Student's t test

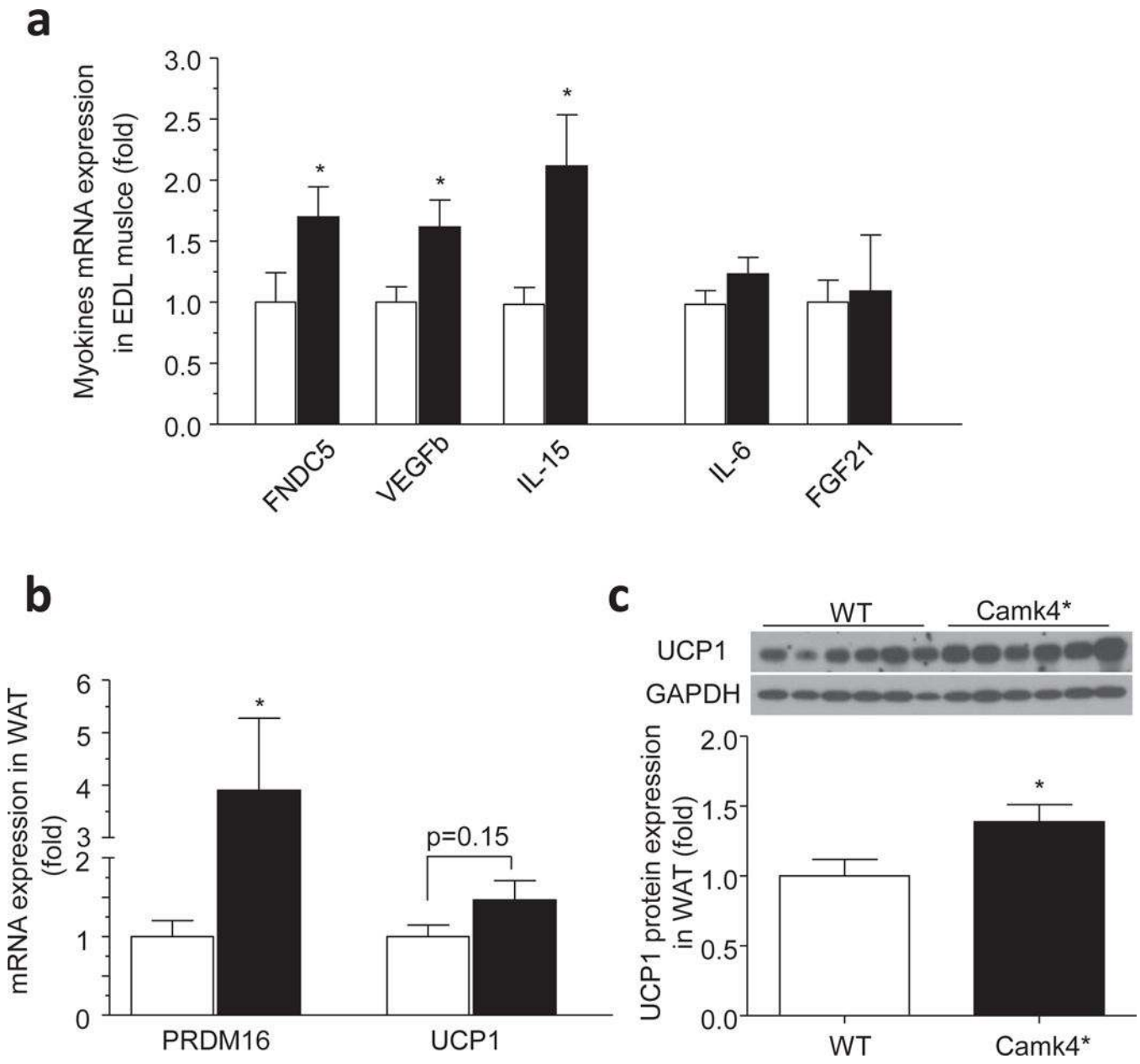

Fig. 5.

Expression of myokines and adipose tissue UCP1 are increased in CAMK4* mice. WT and CAMK4* mice fasted overnight prior to experiments. (**a**) mRNA expression of myokines in EDL skeletal muscle. (**b**) mRNA expression of *Prdm16* and *Ucp1* in WAT. p=0.15 for *Ucp1* WT vs CAMK*. (**c**) Protein level of UCP1 in WAT. n=6–7 per group. White bars, WT; black bars, CAMK4*. *p<0.05 compared with WT by unpaired Student's t test

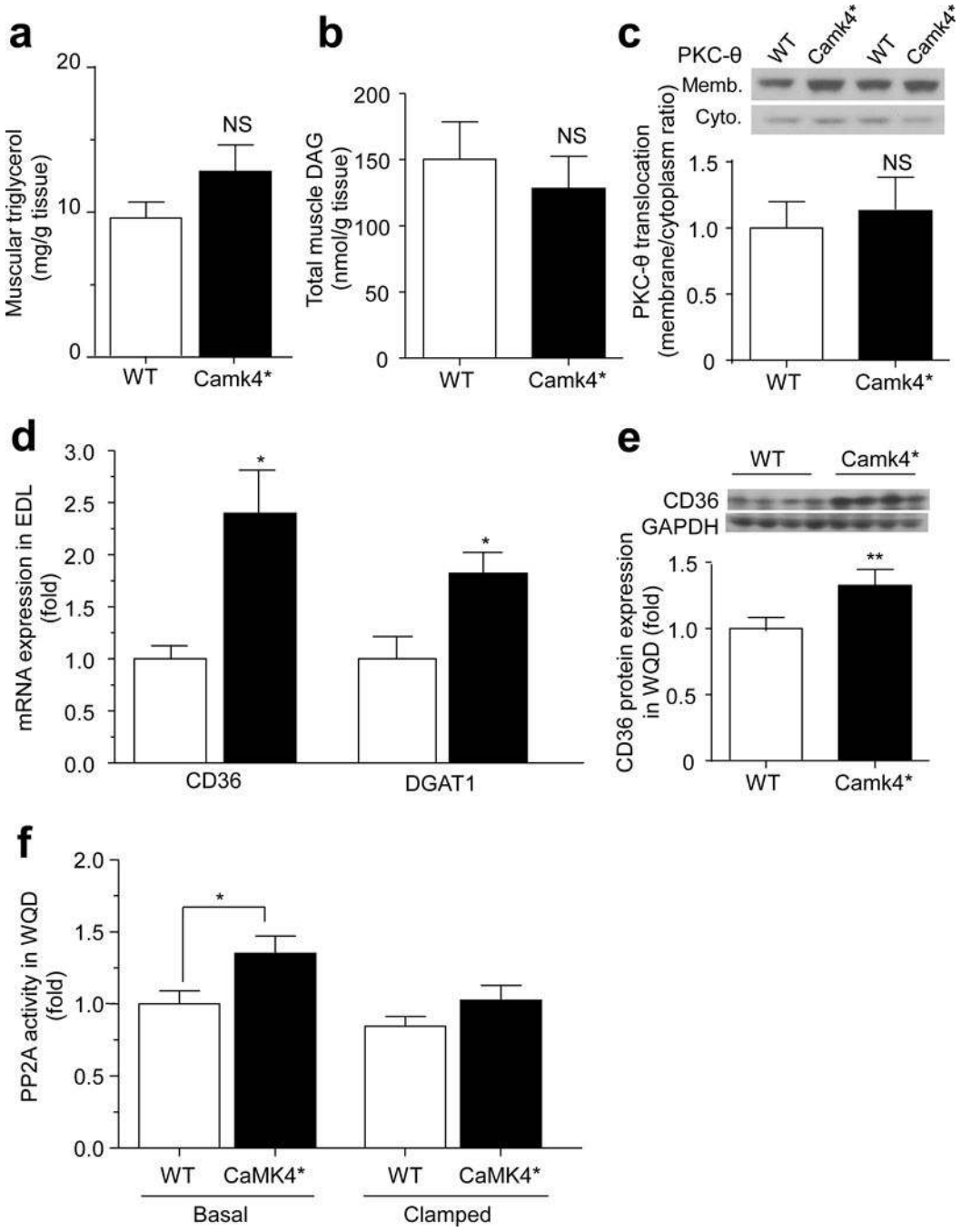

Fig. 6.

Intramuscular lipid accumulation and mRNA expression for fatty acid delivery. (**a**) Intramuscular triacylglycerol and (**b**) DAG accumulation in WQD from CAMK4* and WT mice. (**c**) Representative images and quantification of results of membrane translocation of PKC-θ in WQD muscle. (**d**) Quantitative PCR analysis of mRNA in EDL muscle for CD36 and DGAT1. (**e**) Representative images and quantification of level of CD36 in WQD muscle. (**f**) PP2A activity in WQD from CAMK4* and WT mice. *n*=6–7 muscles per group. White

bars, WT; black bars, CAMK4*. *p<0.05 and **p<0.01 by unpaired Student's t test compared with WT. Cyto., cytoplasm; Memb., membrane

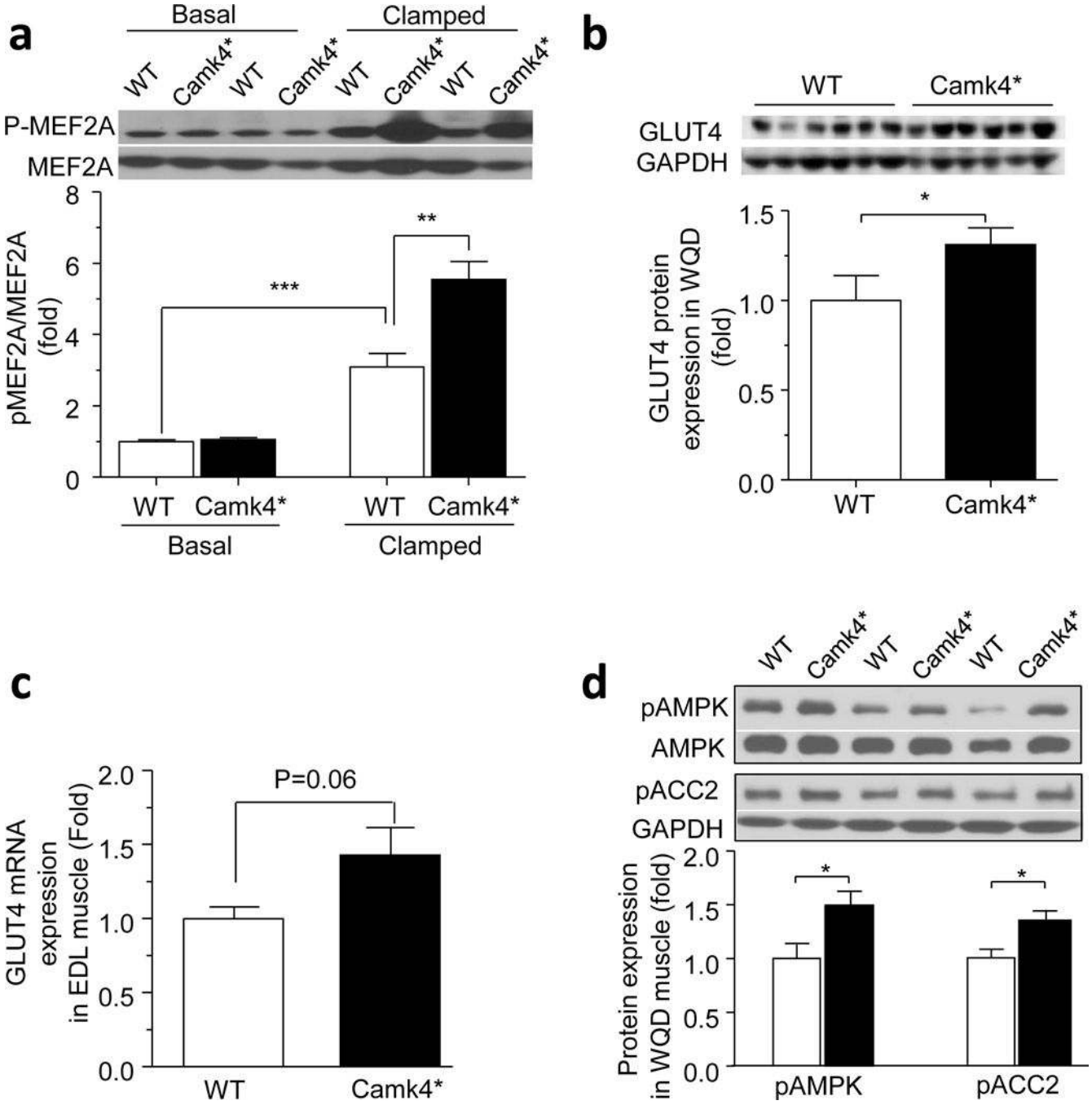

Fig. 7.

Insulin-responsive phosphorylation of MEF2A and PP2A activity. (**a**) Representative images and quantification of results for MEF2A protein levels and phosphorylation in WQD muscle from overnight-fasted (basal) and post-clamped mice (n=7). (**b**) Representative images and quantification of results for GLUT4 protein level in WQD muscle from overnight-fasted CAMK4* and WT mice (n=6). (**c**) mRNA expression of *Glut4* in EDL muscle (n=6); p=0.06 for WT vs CAMK*. (**d**) Representative images and quantification of results for AMPK (Thr172) and ACC2 (Ser219/Ser221) phosphorylation in WQD skeletal muscle from

overnight-fasted WT and CAMK4* mice (n=6–8). White bars, WT; black bars, CAMK4*. *p<0.05, **p<0.01 and ***p<0.001 by unpaired Student's t test

Table 1

Body weight and plasma variables

Variable	WT	CAMK4*
Body weight (g)	31.8 ± 0.8 (n=7)	32.4 ± 0.4 (n=8)
Body fat (%)	10.3 ± 2.1 (n=7)	9.8 ± 1.1 (n=8)
Lean body mass (%)	75.7±2.0 (n=7)	76.0±0.9 (n=8)
Fasting plasma glucose (mmol/l)	6.08 ± 0.23 (n=8)	6.03 ± 0.17 (n=10)
Clamp plasma glucose (mmol/l)	6.52 ± 0.16 (n=8)	6.73 ± 0.14 (n=10)
Fasting plasma insulin (pmol/l)	108.3 ± 13.9 (n=8)	77.1 ± 5.6 (n=10) †
Clamp plasma insulin (pmol/l)	485.5 ± 30.6 (n=8)	500 ± 35.4 (n=10)
Fasting plasma NEFA (mmol/l)	1.01 ± 0.08 (n=8)	1.04 ± 0.07 (n=8)
Clamp plasma NEFA (mmol/l)	0.26 ± 0.05 (n=8)	0.24 ± 0.05 (n=8)
Insulin-suppressed NEFA (%)	73.9 ± 4.8 (n=8)	77.2 ± 4.2 (n=8)

Animals were fed regular chow and fasted overnight for glucose and insulin measurements

Data are expressed as mean values ± SEM

† $p<0.05$ by unpaired Student's *t* test compared with WT